

Partial Dislocation Tutorial for FCC Metals

W.D. Nix, Stanford

Introduction

It is well known that dislocations in FCC metals are composed of partial dislocations separated by stacking faults. When considering the reactions of dislocations with each other, it is necessary to determine the relative positions of the partials in order to correctly describe the configurations that are created in the reactions. Here we describe a geometric method for correctly determining the relative positions of the partials. The results we obtain can also be found by applying an axiom, or rule, given in the book by Hirth and Lothe. At the end of this tutorial we describe this axiom and apply it to some of the problems we have discussed. Our hope is that the geometric method we describe will give readers an intuitive sense of the geometry of partial dislocations and confidence in using the Hirth/Lothe axiom.

Throughout this discussion we will adopt the right-hand, start-finish (RH/SF) convention, wherein the Burgers vector for a given dislocation is found by looking along the sense vector, running one way or the other along the dislocation line, and drawing the Burgers vector from the start of a right-handed Burgers circuit to the finish of that circuit. As a reminder about these vectors, Fig. 1 shows a positive edge dislocation defined by a sense vector and the Burgers vector using the RH/SF convention. Note that the cross product of the sense vector onto the Burgers vector, $\vec{\xi} \times \vec{b}$, points to the “extra half plane” defining this edge dislocation, regardless of which way the sense vector is defined. Figure 2 shows a right-handed screw dislocation with a sense vector and the corresponding Burgers vector, again using the RH/SF convention. For the case of a right-handed screw dislocation the dot product of the sense vector and the Burgers vector, $\vec{\xi} \cdot \vec{b}$, is positive using the RH/SF convention, regardless of which way the sense vector is defined. When the RH/SF convention is used, the sense vector and corresponding Burgers vector completely define the

character of the dislocation (positive edge, negative edge, right handed screw, left handed screw, etc.). We will see that the relative positions of partial dislocations can be determined using this convention and knowledge of how the dislocation responds to a given shear stress.

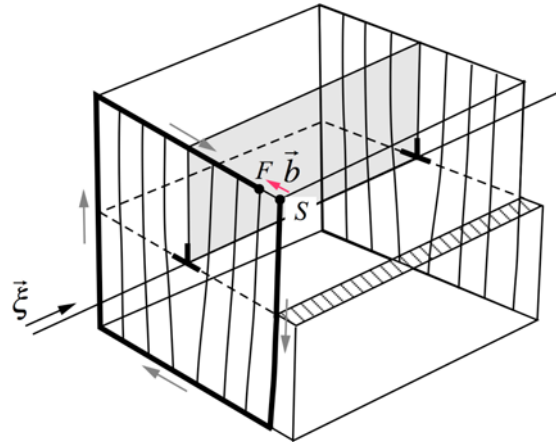


Figure 1. Sense vector and Burgers vector for an edge dislocation using the RH/SF convention.

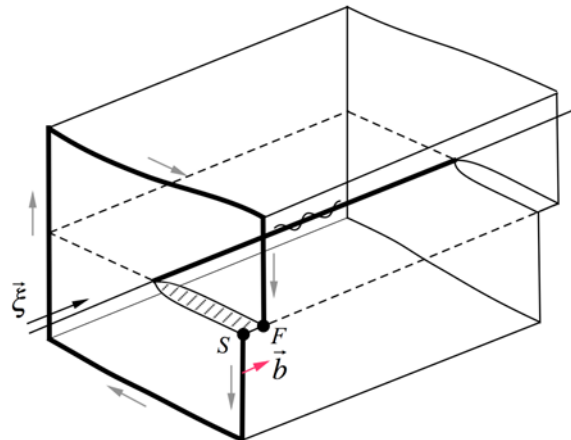


Figure 2. Sense vector and Burgers vector for a right-handed screw dislocation using the RH/SF convention.

Response of a perfect dislocation to a shear stress

We start with a reminder about how a perfect dislocation moves in response to a shear stress. A perfect glide dislocation loop is shown in Fig. 3, subjected to a resolved shear stress that causes it to expand. Using the coordinate system shown, the applied shear stress is $\sigma_{xz} = -\tau$, where τ is the

magnitude of the shear stress. A sense vector is shown for this loop, along with the Burgers vector that would be found using the RH/SF convention. The drawing shows that the character of the dislocation is clearly defined everywhere.

A useful diagram for describing the essential features of Fig. 3 is shown in Fig. 4; it is also called the standard glide loop. This diagram can be used to construct a “hand” rule that can be used to determine the direction of motion of a given dislocation in response to a shear stress. By placing your right hand on the plane of the diagram with your fingers pointing in the shear direction, your thumb correctly points in the direction that a RHS dislocation would move. Similarly, using your left hand with your fingers pointing in the direction of shear, your thumb points in the direction of motion of the LHS. In each case your fingers point in the direction of motion of the positive edge dislocation; the negative edge dislocation moves in the opposite direction. We will use these rules to determine how an extended dislocation moves.

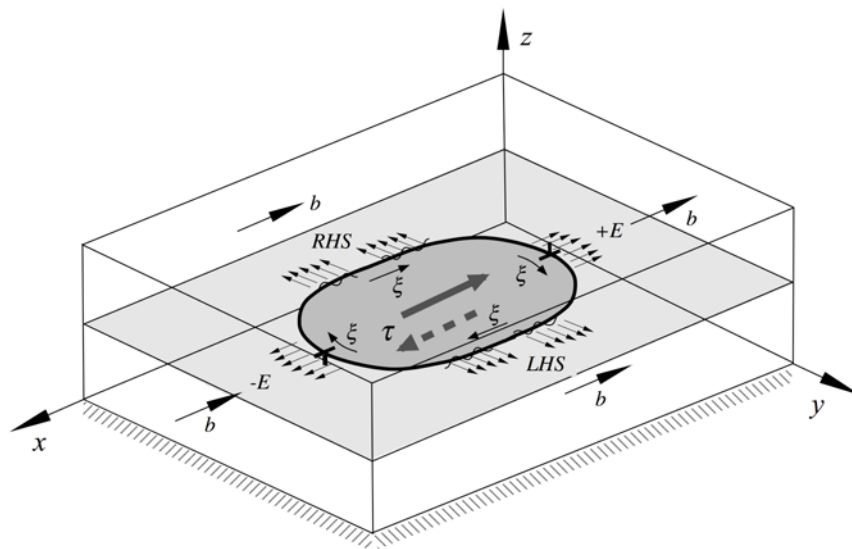


Figure 3. Standard glide loop expanding in response to an applied shear stress, showing a sense vector, ξ and the corresponding Burgers vector, b , (RH/SF convention) which define the character of the dislocation everywhere.

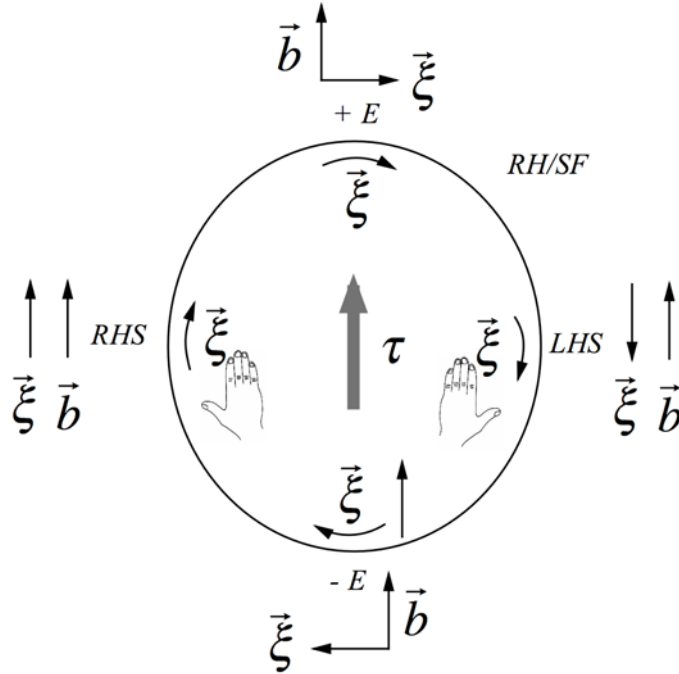


Figure 4. Standard glide loop (that expands under the applied shear stress) showing the relevant vectors. The “hand” rules are illustrated.

Thompson Tetrahedron

We describe partial dislocations using the Thompson notation and the Thompson tetrahedron. Figure 5 shows all the lattice points in an FCC unit cell, as well as some that are outside the unit cell. The four lattice points that make up the Thompson tetrahedron are illustrated with a dark shade: one lattice point located at the origin and three at the centers of the three adjoining faces. These four lattice points form the vertices of the Thompson tetrahedron, also shown in the diagram. The faces of the Thompson tetrahedron coincide with the close packed slip planes in the FCC lattice while the edges of the tetrahedron correspond to the close packed slip directions. The vectors extending from one vertex to another are perfect lattice translations. It is plain from the crystallography that ABC corresponds to the $(1 \bar{1} 1)$ plane and the vector \overline{AC} corresponds to the $a/2[0 \ 1 \ 1]$ translation, for example. All of the other planes and directions implied by the Thompson notation can be determined by reference to the unit cell. The centers of the faces of the tetrahedron are denoted

with Greek symbols corresponding the label of the opposite vertex. These points are not lattice points; they represent faulted atomic positions. As another example, the direction $\overline{A\delta}$ corresponds to the $a/6[1 \ 2 \ 1]$ translation from a lattice point to a faulted position. Having established the connection between the directions and planes in the Thompson tetrahedron and the crystallographic planes and directions, we can use the Thompson notation for all Burgers vectors.

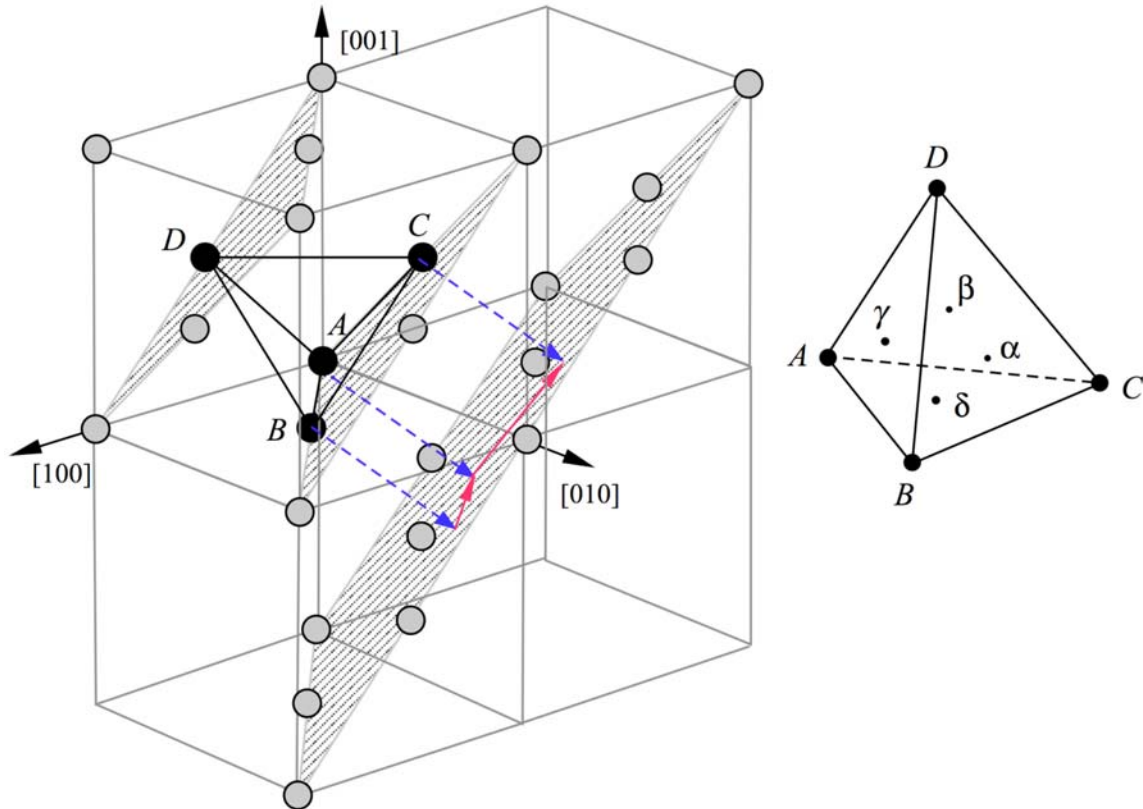


Figure 5. Construction of the Thompson tetrahedron

Slip Occurs on the Inside Surface of the Thompson Tetrahedron, not on the Outside Surface

Consider a unit amount of slip on the $(1 \ \bar{1} \ 1)$ plane (the shaded planes in Fig. 5) and in the closed-packed, \overline{BC} direction. Referring to the unit cell and to the corresponding tetrahedron, one might be tempted to say that an atom initially located at B would first slide to the faulted position δ and then to the final lattice position C , all relative to the atoms in the layer that contains the lattice

point D , in one of the other shaded planes. But if shear of this kind occurred, the atom initially at B would have to ride over the very top of the atom located at D , a highly energetic process. Instead the atom at B slides to δ and then to C relative to the shaded close packed layer outside of the tetrahedron. Thinking of the tetrahedron as a solid object, we say that atoms cannot slide from B to δ to C on the outside surface of the tetrahedron because that would result in the atoms riding up over the tops of the atoms below (in layer D). Instead, all of the atoms in the tetrahedron slide together relative to the atoms outside of the tetrahedron. We can think of atoms sliding on the inside surface of the tetrahedron relative to the atoms outside the tetrahedron. The blue arrows indicate the positions taken as atoms slide from B to δ and then to C on the plane outside of the tetrahedron.

Figure 6 shows another illustration of “sliding on the inside surface of the tetrahedron.” Here the Thompson tetrahedron is positioned between two “slip pyramids.” The red arrows indicate that slip occurs on the outside surface of the slip pyramid (equivalent to the inside surface of the tetrahedron). The diagram shows that when atoms slide from B to δ they do so by moving to the midpoint of the three atoms on the shaded plane below.

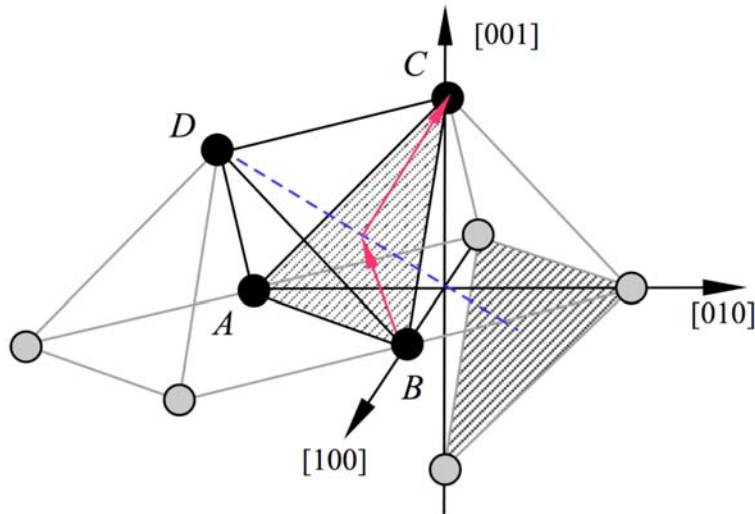


Figure 6. Slip pyramids separated by a Thompson tetrahedron, showing that slip on the *inside surface of the tetrahedron* is equivalent to slip on the *outside surface of the slip pyramid*.

A Simple Example

Consider a negative edge dislocation with Burgers vector $b = BC$ gliding on the ABC plane, as shown in Fig. 7. Henceforth we will drop the arrows in \overline{BC} and take BC to mean the translation from the lattice point B to the lattice point C . In this illustration, and ones to follow, we make use of the Thompson tetrahedron to describe common Burgers vectors and slip planes and also use the diagram to show the possible arrangements of dislocations and their reactions. Thus the Burgers vector diagram and the dislocation line diagram will be superimposed. We wish to determine the character of the leading and trailing partial dislocations for the dislocation shown. We impose a shear stress that would cause sliding “on the inside of the Thompson tetrahedron” in the direction of the Burgers vector, as shown. We then ask how the edge would move in response to that shear stress. Using the “hand” rules discussed above (either hand can be used for the edge), we find that the negative edge would move in the direction from C to B . This means that the leading partial (the first one to arrive at a given point in the crystal) is closest to B and the trailing partial is closest to C , as shown. The blue arrows are the sense vectors for the Burgers vectors shown.

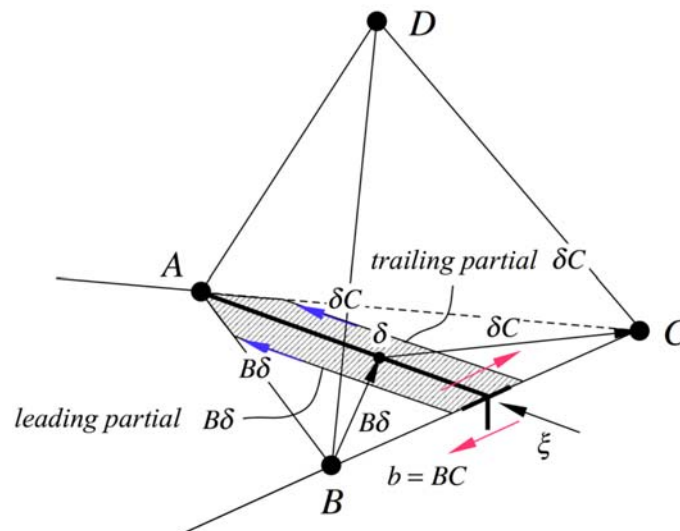


Figure 7. Glide of a negative edge dislocation.

Other Simple Examples

Consider a left-handed screw gliding on the ABC plane as shown in Figure 8. For the given sense vector, the Burgers vector is $b = CB$. So we impose a shear stress on the “inside surface of the tetrahedron” and observe, using the left “hand” rule that the LHS moves from the line BC toward the point A . This means that the partial nearest A is the leading partial, with Burgers vector $C\delta$, while the trailing partial is nearest the line BC , with Burgers vector δB .

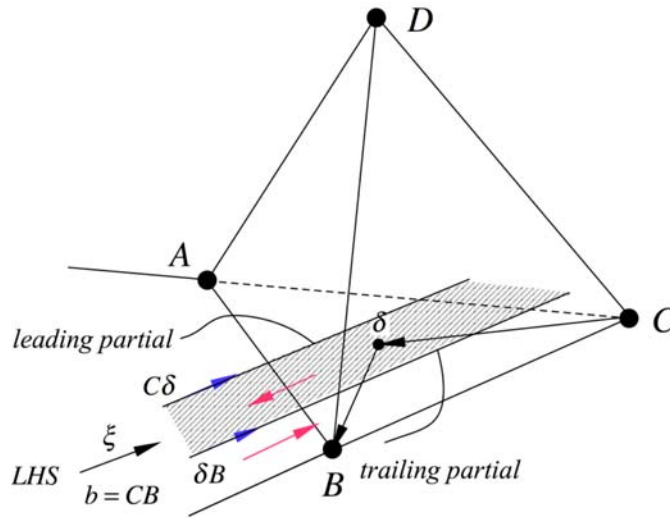


Figure 8. Partials in a left handed screw.

Since the Burgers vectors depend on the choice of the sense vector, it may be worthwhile to illustrate the LHS glide problem using a different choice for the sense vector, as shown in Fig. 9. For this sense vector the Burgers vector is $b = BC$, so we again impose a shear stress on the “inside surface of the tetrahedron” in the direction of the Burgers vector and, using the left “hand” rule, observe that the partial nearest the line BC is now the leading partial with Burgers vector $B\delta$ while the trailing partial has the Burgers vector δC . We note that the structure of the dislocation in Fig. 9 is identical to that in Fig. 8, as expected.

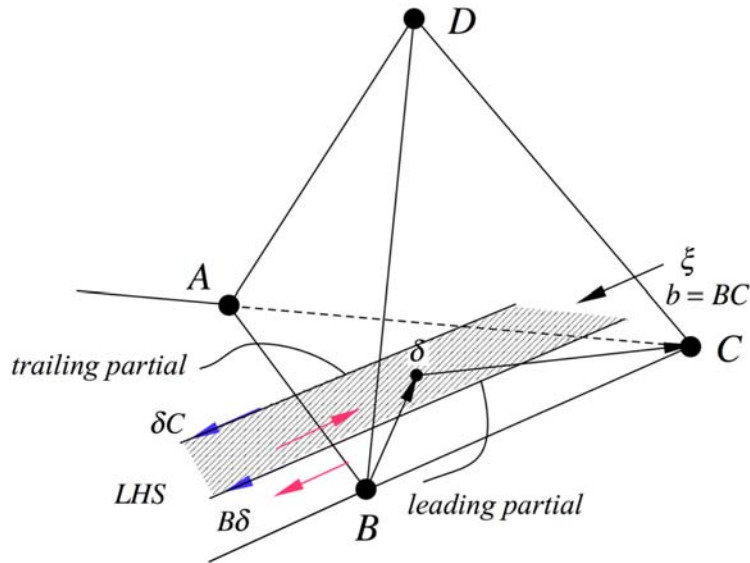


Figure 9. Partial in a left handed screw (with a different sense vector).

Lomer-Cottrell Dislocation

The rules we have developed have implications for the structure of the Lomer-Cottrell dislocation, which we consider now. Consider two 60° dislocations, one with Burgers vectors $b = BC$ (for the sense vector shown) gliding on the ABC plane and another with Burgers vector $b = DB$ gliding on the ABD plane. These two dislocations will spontaneously react or combine to form a Lomer dislocation with Burgers vector $b = DB + BC = DC$. Each gliding dislocation is separated into partials with Burgers vectors $b = DB + BC = (D\gamma + \gamma B) + (B\delta + \delta C) = DC$. We wish to determine the character of the Lomer-Cottrell dislocation after the reaction. The use of the “hand” rules described below requires that we first decompose the mixed, 60° dislocations into their edge and screw components. The resulting edge components of these dislocations are shown in the diagrams and they can be used to judge to direction of motion for a given shear stress.

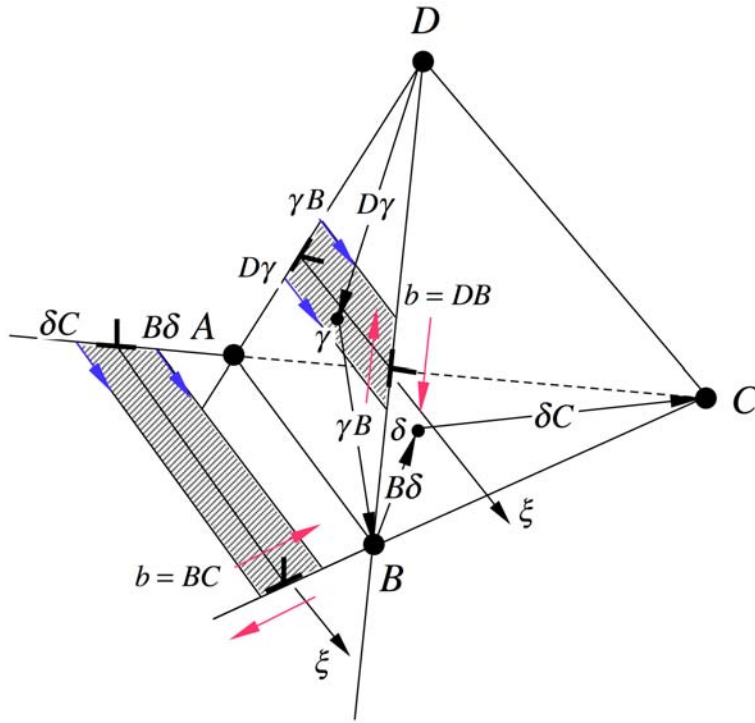


Figure 10. Two 60° dislocations ready to form a Lomer-Cottrell dislocation.

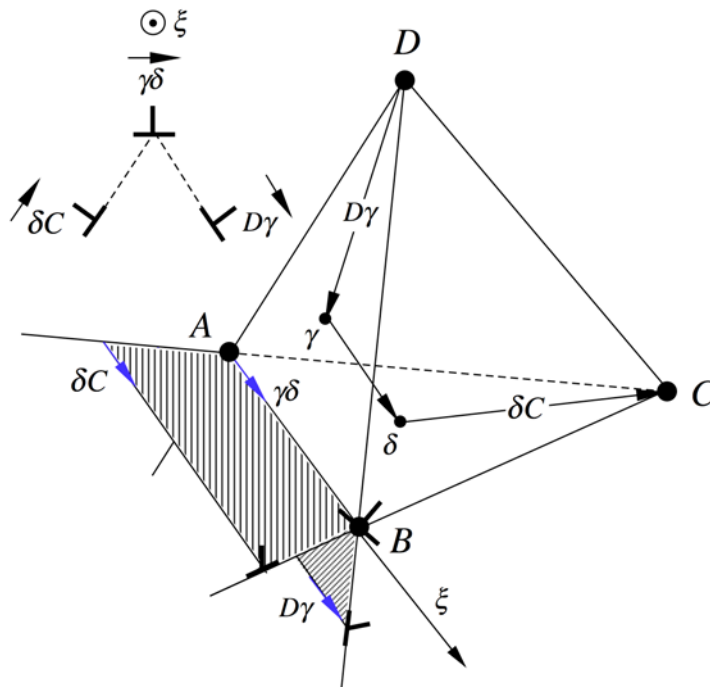


Figure 11. The Lomer-Cottrell dislocation formed by the reaction of two 60° dislocations in Fig. 10.

By imposing shear stresses on the “inside surface of the tetrahedron” in the direction of the Burgers vectors and using the “hand” rules to determine the direction of motion of the two dislocations (focusing mainly on the edge components), we can determine the Burgers vectors of the partial dislocations as shown in Figure 10. The vector notations near the blue arrows indicate the correct results. When these two dislocations come into close proximity, two of the partials will react to form a Stair-Rod dislocation: $\gamma B + B\delta = \gamma\delta$. When the Stair-Rod dislocation is formed along the line of intersection of the two slip planes, the other two Shockley partials, δC and $D\gamma$, take the positions shown. We note that the final structure of the Lomer-Cottrell dislocation involves “diverging extra half planes,” as shown in the inset in Fig. 11. This is the correct structure for the Lomer-Cottrell dislocation. Some references show the extra half planes converging, which is wrong. This structure is a consequence of the “slip on the inside surface of the tetrahedron” rule.

Jogged Dislocation

The rules we have developed can be used to find the structure of any dislocation configuration. Consider first a pure edge dislocation with a jog in the form of a Lomer dislocation, as shown in Fig. 12.

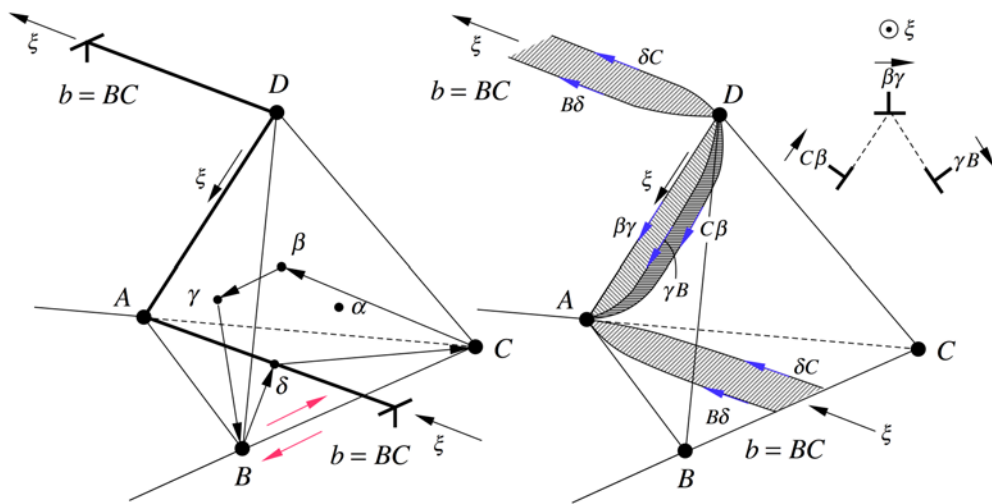


Figure 12. A jogged edge dislocation, before and after extension into partials. Segment AD is a Lomer dislocation.

Imposing a shear stress on the “inside surface of the tetrahedron” on the plane ABC and in the direction of the Burgers vector $b = BC$ allows us to determine that the edge dislocation would glide toward the point B ; this means that the leading partial dislocation for this shear would be $B\delta$ and the trailing partial would be δC , as shown. The partial Burgers vectors for the Lomer-Cottrell dislocation segment are assigned using Fig. 11 as guide.

We now consider the extension of the nodes or corners of this dislocation. We note that partial dislocations $B\delta$ and γB will coincide along the line AB forming a Stair-Rod dislocation: $B\delta + \gamma B = \gamma\delta$. Similarly the partials $C\beta$ and δC will meet along the line AC to form another Stair-Rod dislocation: $C\beta + \delta C = \delta\beta$. The result is that the node at A extends in the manner shown in Fig. 13. The nodal point A then becomes part of a stacking fault tetrahedron. Similar extensions do not occur at the node D because the partial dislocations are not able to coincide along common lines and form Stair-Rod dislocations.

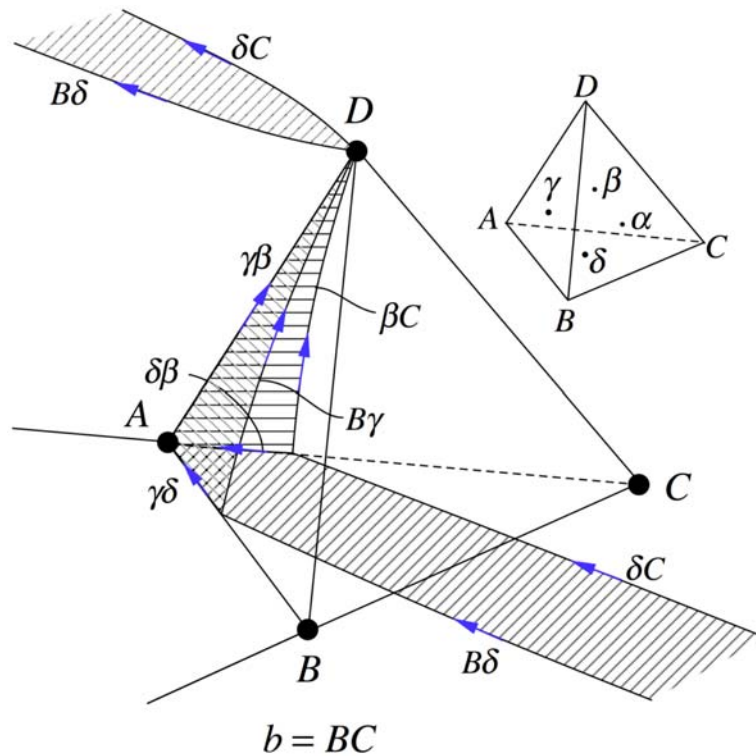


Figure 13. Jogged edge dislocation with an extended node.

As the glide dislocations rotate about on their slip planes the node D will always remain constricted while the node A will become alternately constricted and extended, depending on the orientation of the gliding segments. Figure 14 shows the jogged dislocations after the arms have rotated by 180° . We see that both nodes are constricted in this orientation.

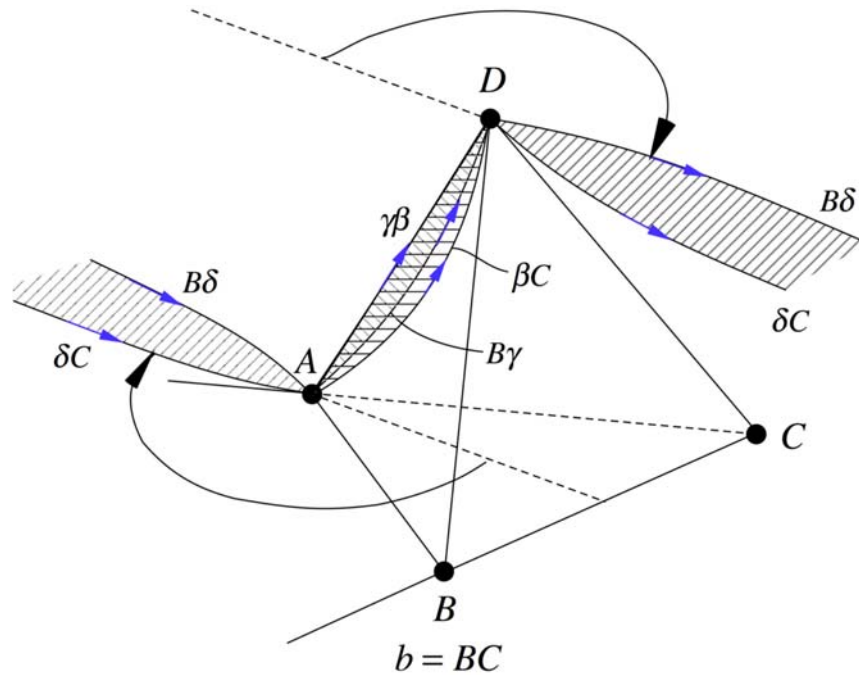


Figure 14. Jogged edge dislocation in a configuration where both nodes are constricted..

We also observe that when the upper gliding arm is positioned mid-way between the positions shown in Figs. 13 and 14, a strong line tension force acts on the node at D , pulling that node in the direction BC . Since the Lomer-Cottrell dislocation is constricted at that node it might be able to glide on the cube plane without much need for thermal activation. This suggests that the Lomer-Cottrell junction might not be as immobile as commonly thought. While the extended part of the Lomer-Cottrell dislocation is expected to be highly immobile because of its non-planar structure, the same cannot be said for the constricted node.

Hirth/Lothe Axiom

As noted in the introduction, all of the results we have described and explained can be found using an axiom given in the book by Hirth and Lothe. We refer to Axiom 10-1 given on page 302 of the first edition of that classic book. The axiom can be restated as follows:

Consider a dislocation with Burgers vector $\overline{AB} = \overline{A\delta} + \overline{\delta B}$ (again using the RH/SF convention) on the ABC plane. Define a unit vector, \vec{n} , normal to the plane ABC that points toward the center of the Thompson tetrahedron. Then $\vec{n} \times \vec{\xi}$ is another unit vector that points to the location of the “first” partial: $\overline{A\delta}$. The other partial, $\overline{\delta B}$, is found in the opposite direction.

We can apply this axiom to obtain the results given in the figures. For example, the Burgers vector in Fig. 7 is $\overline{BC} = \overline{B\delta} + \overline{\delta C}$. The axiom states that the “first” partial, $\overline{B\delta}$, should be in direction $\vec{n} \times \vec{\xi}$, the position shown. For Fig. 8 the Burgers vector is $\overline{CB} = \overline{C\delta} + \overline{\delta B}$. There we find that again $\vec{n} \times \vec{\xi}$ points to the “first” partial, $\overline{C\delta}$. In this way the Hirth/Lothe axiom can be used as a rule to determine the locations of the partial dislocations. The structure of the Lomer-Cottrell dislocation and the extended nodes follows from this rule in the ways shown in the tutorial

Conclusion

The geometric method described here can be used to correctly determine the relative positions of partial dislocations in FCC crystals. The Hirth/Lothe axiom can also be used to obtain these results.